IEEE Access
Multidisciplinary : Rapid Review : Open Access Journal

Received 8 September 2022, accepted 17 September 2022, date of publication 20 September 2022, date of current version 29 September 2022.

Digital Object Identifier 10.1109/ACCESS.2022.3208108

RESEARCH ARTICLE

# Traffic Sign Detection Based on Driving Sight Distance in Haze Environment

**RONG HU, HUI LI, DAN HUANG, XIAOJIN XU, AND KUANGYUAN HE**
Department of Automobile and Transportation, Xihua University, Chengdu 610039, China

Corresponding author: Hui Li (0120050020@mail.xhu.edu.cn)

This work has been supported by the key project of xihua university University, ''Research on Dangerous Scenes of Autopilot in Freeway for Vehicle-Road Cooperation''. Fund No. Z211005.

**ABSTRACT** To explore the relationship between traffic sign detection performance and driving sight distance in haze environment, this paper proposed a UV correlation model among sight distance, haze grade and traffic sign detection performance. First, the German traffic sign data set (GTSDB) is synthesized into experimental data set according to three levels of light haze, haze and dense haze. The Faster R-CNN model is utilized to detect the traffic signs after dehazing by Guided Filter Dehazing Algorithm. The detection accuracy is as high as 95.11%, which shows that the model has strong generalization ability and adaptability. Second, the weight is determined by haze, taking the driving sight distance as U layer and the detection result of Faster RCNN model as V layer, establishing the UV correlation model. Finally, KM algorithm is used to solve the correlation model, and the best matching result between UV layers is gained. The experimental results show the haze level significantly affects the driving sight distance, and then affects the detection accuracy of traffic signs. When the driving Sight distance threshold is 300 meters, 100 meters and 50 meters in light haze, haze and dense haze, the KM algorithm obtains the detection accuracy levels of A (higher than 93%), B (88%-93%) and C (85%-88%), respectively.

**INDEX TERMS** Driving sight distance, faster R-CNN, haze environment, traffic sign detection, UV correlation model.

## I. INTRODUCTION

Road signs are the basic facilities to guide road users to use the road orderly, inform road users of the right of way, and announce road conditions and traffic conditions [1]. Accurate and efficient detection of traffic signs is of great significance to ensure the safety of autonomous vehicles. However, in the haze environment, the line-of-sight is disturbed, which shortens the driving sight distance. It brings significant challenges to detect the traffic signs. The research of autonomous vehicle traffic sign recognition and detection mainly adopts machine learning, deep learning and other methods. With the development of deep learning theory, the improvement of CNN,VGG,YOLO and other neural networks has been widely used in traffic sign recognition and detection [2], [3], [4], [5], [6], [7], [8], [9].

The associate editor coordinating the review of this manuscript and approving it for publication was Shaohua Wan.

Tabernik [2] used Mask-RCNN to detect and recognize large-scale traffic signs. The improved method is employed to experimental evaluation, and the error rate is less than 3%. Wang [3] obtained a model that can classify traffic signs through Caffe, and enabled it to recognize traffic signs in real scenes. Yuanyuan [4] improved the VGG16 network to detect small and dense traffic signs. Qiyuan [5] based on the improved YOLOV3, detects traffic signs in complex environments. The idea of residual dense network is used to realize the reuse and integration of multi-layer features of the network. Arman [6] proposed a new lightweight CNN architecture. Measure based on GTSRB and BTSCD datasets, and retrain the network model using transfer learning. Hechri and Mtibaa [7] uses HOG features and SVM to classify traffic signs and recognize them through a convolutional neural network. Wang [8] proposed improving the accuracy of traffic sign recognition based on a deep cascade network with cascaded sub-networks. The speed sign detection based on a complex environment has achieved good experimental results. Zhang *et al.* [9] proposed a cascaded R-CNN to obtain multi-scale features of pyramids to detect traffic signs. Then the detection accuracy is enhanced by multi-scale attention and data expansion. The method is used in GTSDB, CCTSDB and reliable experimental results have been achieved in datasets such as LISA.Besides improving the model, many scholars also put forward innovative experimental methods to identify and detect traffic signs [10], [11], [12], [13], [14], [15], [16], [17], [18], [19], [20] Li and Wang [10] designed and implemented a detector using the framework of Faster RCNN and the structure of MobileNet. Arcos-García *et al.* [11] proposed a deep learning method for traffic sign recognition system. Li *et al.* [12] put forward the deep learning method of DeepSign to study the task of traffic sign recognition. Zhang *et al.* [14] put forward TSR algorithm on the basis of improving LeNet-5 algorithm. Aziz and Youssef [17] proposed a novel and effective traffic sign recognition method based on the combination of complementary feature set and discriminant feature set. Nadeem *et al.* [18] proposed a method around deep learning. Firstly, the model was pre-trained on the German traffic sign data set. And then the model was fine-tuned using the Pakistani data set (359 different images). The models proposed by these scholars have obtained excellent experimental results, which can efficiently and accurately detect and identify traffic signs. Cao *et al.* [19] proposed an improved sparse R-CNN model, and further improved the existing backbone network. Experiments on TT100K data set show that this method has good accuracy and robustness. Ren *et al.* [20] proposed a new type of real-time traffic sign detection system, which uses deep separable DetNet(DS-DetNet) lightweight backbone network and lightweight feature pyramid network (LFFPN) to realize feature fusion.

The above research is mainly aimed at the visual recognition of autonomous vehicles in normal driving environment. At present, research on traffic sign recognition and detection in special environments such as haze has attracted notable attention [21], [22], [23], [24], [25], [26], [27], [28], [29], [30]. Hodges [21] used Siamese network to create a new training method of image dehaze model based on deep learning. The model achieves superior performance with multiple image quality metrics, as well as improvements in object detection. Yan *et al.* [22] used a dark channel priors and support vector machines to dehaze and classify speed limit signs. A seven-layer convolutional neural network is employed for identification. The recognition rate of the model for speed limit signs is 98.51%, which is better than human performance. Xinxiu *et al.* [23] used IRCNN to remove the haze. A multi-channel convolutional neural network model is proposed to recognize dehazed images. And its recognition effect is common and its adaptability is strong. Wiesemann and Jiang [24] studied the effect of haze on traffic sign detection and simulated the visibility using a haze model, validating the performance of the detection method. Ma *et al.* [26] used dark channel prior algorithm based on guided filtering to process foggy images, and detected them based on improved YOLOv3 detection algorithm. Anthony and Biswas [27] used machine learning technology and convolutional neural network to realize real-time traffic sign detection in fog.

In the haze environment, the driving sight distance has a significant impact on the detection and recognition of traffic signs. Deng *et al.* [31], based on limited sight distance, used hierarchical driving behavior assessment to observe dangerous driving behavior in haze. The experimental results can inform actions to improve road safety during heavy haze. Belaroussi and Gruyer [25] produced images of traffic signs including haze and no haze. And according to the density of haze to measure the distance required to detect the marker and the meteorological visibility distance and its influence on safety. Discetti and Lamberti [32] specially developed a mathematical model to study the relationship between sight distance and sign position. The warning curve of insufficient sight distance was investigated.

In order to verify the detection performance of traffic signs in haze environment, the relationship between driving sight distance, haze level and detection clarity of traffic signs is comprehensively considered. We established a UV correlation model. KM algorithm is introduced into traffic sign detection experiment for the first time to discuss the relationship between sight distance, haze level and traffic sign detection effect. In addition, different from other papers on haze removal, we study the haze degree in different grades, and the comparative experiment can reduce the experimental error to a certain extent. Using the guided filtering algorithm to improve the traditional dark channel prior theory, it can not only remove haze efficiently, but also remove the noise on the image. Faster R-CNN model is used to detect traffic signs on the haze-removed images. Based on the experimental results, the influence of different sight distances on traffic sign detection in haze environment is discussed.The main contributions of this paper are as follows:

(i) In order to avoid experimental errors, this paper studies the classification and refinement of haze. Based on the prior theory of dark channel, the guided filter is used to improve it. The improved method can not only remove the haze of traffic signs, but also eliminate the bad phenomena such as white edge and halo effect, and denoise the images.

(ii) The UV correlation model established in this paper can well explore the relationship between haze, traffic signs and the threshold of sight distance. This paper applies KM algorithm to traffic sign detection for the first time. KM algorithm is used to analyze and solve the proposed UV model. Finally, the influence level of sight distance threshold on traffic sign detection effect in haze environment is obtained.

(iii) he experimental method adopted in this paper is quick and simple, and can be extended to other data sets.

The experimental process is illustrated in Figure 1.

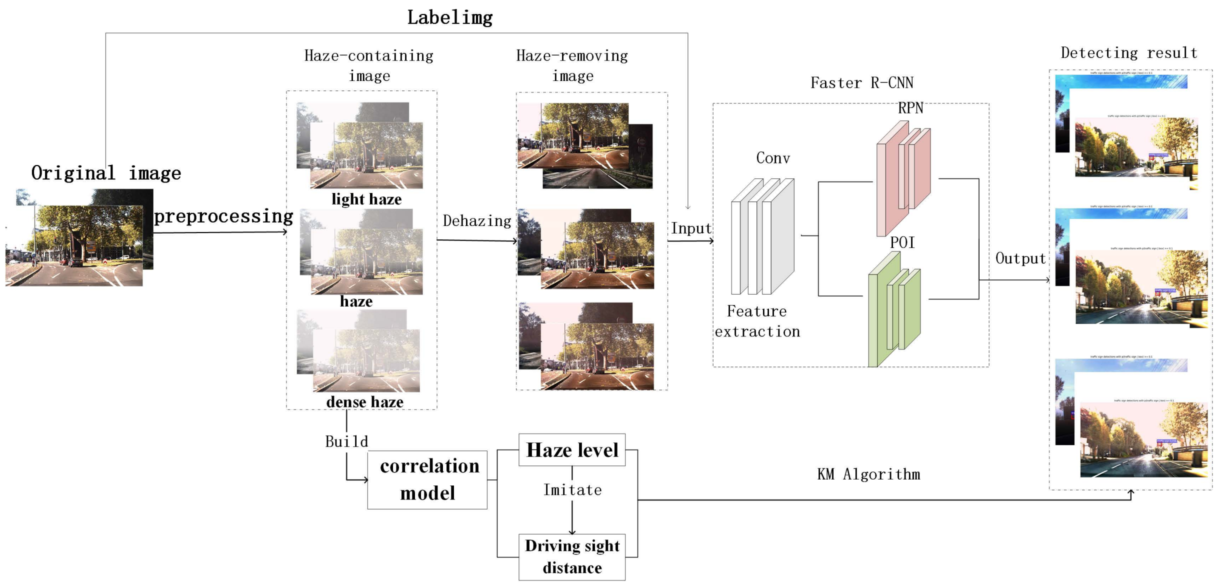


**FIGURE 1.** Experimental modeling process.

## II. MODEL ESTABLISHMENT

### A. DEHAZING MODEL

#### 1) ATMOSPHERIC SCATTERING MODEL

In computer vision, atmospheric scattering models are widely used:

$$I(X) = J(X)t(x) + A(1 - t(X)) \tag{1}$$

Among them, $I(X)$ is the image to be dehaze, $J(X)$ is the image to be restored without haze, A represents the global atmospheric light component, and $t(x)$ is the transmittance. The current known condition is $I(X)$ and the target value $J(x)$ is required. The three unknowns make the equation have infinite solutions, so a prior is required.

#### 2) DARK CHANNEL PRIOR ALGORITHM

Hek *et al.* [33] experimental teams proposed a dark channel prior model to perform statistical analysis on a large number of haze-free images. Then, the haze distribution is estimated based on the atmospheric scattering model. Satisfactory defogging effect is obtained.

The dark channel means that in the local area of most images, one or more of the three color channels of R, G, and B have gray values with some pixels that are very small or even close to 0. For any input image, the size of the dark channel of the point value can be solved by the following formula:

$$J_{\text{dark}}(x) = \min_{y\in\Omega(x)}\left[\min_{c\in\{r,g,b\}} J^c(x)\right] \tag{2}$$

Among them, $\Omega(x)$ is the local area centered on $x$ in the input image, $J^c(x)$ is the gray value of one channel in the corresponding image area, and $J_{dark}(x)$ is the minimum value of a pixel in the three channels of R, G and B. The dark channel prior theory points out that the dark channel of the output haze-free image $J(x)$ tends to zero for non-sky areas. According to the atmospheric scattering model, assuming that the atmospheric light value $A$ is known, the formula (1) is transformed to obtain:

$$\frac{I^C(x)}{A^C} = t(x)\frac{J^C(x)}{A^C} + 1 - t(x) \tag{3}$$

The transmittance $t(x)$ of each window is assumed to be a constant and recorded as $\tilde{t}(x)$. When the value of A is known, the minimum value of both sides of equation (3) can be obtained twice at the same time.

$$\min_{y\in\Omega(x)}\left[\min_{c}\frac{I^C(x)}{A^C}\right] = \tilde{t}(x)\min_{y\in\Omega(x)}\left[\min_{c}\frac{J^C(x)}{A^C}\right] + 1 - \tilde{t}(x) \tag{4}$$

According to the dark channel prior theory:

$$J_{\text{dark}}(x) = \min_{y\in\Omega(x)}\left[\min_{c\,\in\,\{r,\,g,\,b\}} J^c(x)\right] = 0 \tag{5}$$

Substitute equation (5) into equation (4) to get the estimated value of transmittance $t$.

$$\tilde{t}(x) = 1 - \min_{y\,\in\,\Omega(x)}\left[\min_{c}\frac{I^C(x)}{A^C}\right] \tag{6}$$

In real life, smog is everywhere. Even on sunny days, there is still some particulate matter in the air. Therefore, in order to ensure the depth of field of the human eye, it is necessary to maintain a certain degree of haze during dehazing. The estimated transmittance are corrected by introducing a factor between 0 and 1 (typically $w = 0.95$), as shown in equation (7):

$$\tilde{t}(x) = 1 - \omega\min_{y\,\in\,\Omega(x)}\left[\min_{c}\frac{I^c(x)}{A^c}\right] \tag{7}$$

When the atmospheric light value A is unknown, the dark channel algorithm can effectively remove haze. By in the original haze image, the extracted pixels are 0.1% before the brightness, and then the atmospheric light value A is set as the highest brightness point value in the input image. To avoid that the transmittance is too small to cause the haze-free image to be excessively white, the lower limit value of transmittance $t_0$ is taken as 0.1. When $t < t_0, t = t_0 = 0.1$. The transmittance and atmospheric light value are substituted into formula (1), and the restoration formula of the sorted image is as follows:

$$J\left(x\right)=\frac{I\left(x\right)-A}{max[t\left(x\right),t_0]}+A \tag{8}$$

#### 3) GUIDED FILTER DEHAZING ALGORITHM

Because the calculated transmittance is relatively rough, the image effect obtained only by the above method is difficult to meet the experimental needs [34]. To effectively avoid the white edge and halo effects, the method of guided filtering is used to improve the dark channel prior algorithm by refining the transmittance map. Suppose the image is a two-dimensional function that cannot be expressed analytically, so the input and output of the function satisfy the following linear relationship in the two-dimensional window:

$$q_i=a_kI_i+b_k\ \left(\forall i\in w_k\right) \tag{9}$$

where $q$ and $i$ are the output pixel and input image values, respectively, $I$, $k$ are the pixel indices, and $a$ and $b$ are the coefficients of the linear function when the window center is at $k$. Equation (9) can effectively remove image noise.Taking the gradient on both sides of the above equation, we can get:

$$\nabla_q=a\nabla \mathrm{I} \tag{10}$$

Next, find the linear regression coefficients and minimum values of the following formulas:

$$E\left(a_k,b_k\right)=\sum_{i\in wk}\left(\left(a_kI_i+b_k-p_i\right)^2+\in {a_k}^2\right) \tag{11}$$

By the least square method, we can get:

$$a_k=\frac{\frac{1}{|w|}\sum_{i\in w_k}\left(I_ip_i-u_k\widetilde{p}_k\right)}{\sigma_k^2+\in} \tag{12}$$

$$b_k=\widetilde{p}_k-a_ku_k \tag{13}$$

where $u_k$ is the average value in window $w_k$, ${\sigma_k}^2$ is the variance in window, $|w|$ is the number of pixels in the window, and $\widetilde{p}_k$ is the mean of the image $p$ in the window $w_k$ to be filtered.

Calculates the average of all linear function values at a point. The output value at this point can be obtained:

$$q_i=\frac{1}{|w|}\sum_{i\in wk}\left(a_k+b_k\right)=\bar{a}_iI_i+\bar{b}_i \tag{14}$$

This method can achieve edge preservation and smoothing effects. Its processing time is relatively short, so it has strong practicability. Its greatest advantage is to make the output and input images as gray as possible. At the same time, it is ensured that the gradient of the output image is similar to that of the guide image, to retain the essential characteristics of the image.

Dehaze using an improved dark channel dehazing algorithm. The treatment effect is shown in Figure 2. Among them, Figure 2 contains three different levels of haze renderings of light haze, haze and dense haze. As the haze increases, the visibility of traffic signs becomes worse due to the enhanced line-of-sight interference. The sharpness of the dark primary color image decreases as the haze increases. After the image is dehazed, the recognition clarity of the traffic sign image is enhanced, which is beneficial to the visual recognition and driving safety of autonomous vehicles.

Figure 2 Subjectively evaluates the experimental results of haze removal by guided filtering. Table 1 objectively evaluates the experiment. By comparing the peak signal-to-noise ratio (PSNR) and structural similarity (SSIM) of the dark channel haze removal experiment and the guided filter haze removal experiment, it can be seen that the experimental results of the guided filter haze removal algorithm under the conditions of light haze, haze and thick haze are better than those of the dark channel prior haze removal experiment.

**TABLE 1.** **Comparative evaluation of two dehazing algorithms.**

| | PSNR | | SSIM | |
|---|---|---|---|---|
| | dark channel | guide filter | dark channel | guide filter |
| light haze | 25.6389 | 28.8428 | 0.7653 | 0.8767 |
| haze | 22.5271 | 28.2237 | 0.6989 | 0.8021 |
| dense haze | 19.2995 | 24.8029 | 0.6342 | 0.7045 |

### B. TRAFFIC SIGN DETECTION MODEL

#### 1) FASTER-RCNN

Traditional detection frame generation process is slow. Adaboost [35] uses a combination of sliding window and image pyramid to complete the detection frame generation. SS (Selective Search) method is used to generate detection boxes in RCNN. In contrast, Faster R-CNN [42] improves on its drawbacks. The RPN network is therefore proposed replacing the traditional candidate region generation method. The sliding window and SS method are removed to realize end-to-end training. Meanwhile, RPN and Fast R-CNN share convolutional features, which greatly reduce the training time. ROI (Region of Interest) pooling uses max pooling to fix the ROI on the feature map and thus the feature map size. Use NMS (Non-maximum Suppressing) technology to filter the number of candidate frames to get the highest detection result.

To speed up extracting candidate regions and overcome the problem of poor robustness of artificially designed features, this paper uses the Faster R-CNN model in object detection. The RPN is used to generate proposal candidate regions. The detection network is utilized to classify and locate pedestrian objects. The traffic sign detection process is illustrated in Figure 3, where Faster R-CNN includes RPN


**FIGURE 2.** **Comparison of dehazing performance with different haze.**

and detection network. The whole process of traffic sign detection is divided into input image, calculation of convolution features through VGG16, extraction of initial candidate regions. The RPN is used to generate more accurate candidate regions, and the detection network is used for classification and regression calculation to obtain the rectangular frame of traffic signs.

### 2) DETECTION AND TRAINING

The RPN network is transferred to the ROI pooling layer for pooling operation, and a fixed-size candidate region feature map is generated. Classification and bounding box prediction are performed on these features. The detection network has two parallel output layers. The output of the classification layer is the probability distribution $p = (p_0, p_1)$ of each bounding box over the two classes of traffic signs and non-traffic signs. Output of the border regression network is the border position parameter, $t^k = (t_x^k, t_y^k, t_{xw}^k, t_{xh}^k)$, and k represents the category. The bounding box regression network and bounding box classification network is trained by a joint loss function, namely.

$$L\left(p, u, t^u, v\right) = L_{\mathrm{cls}}(p, u) + \lambda[u \geqslant 1] \cdot L_{\mathrm{reg}}\left(t^u, v\right) \quad (15)$$

where $L_{cls}(p, u) \;=?log(p_u)$ is the logarithmic loss of true category $u$. $Lreg$ will only be activated when the area to be detected is a traffic sign, that is, $p * i = 1$. In order to get accurate rectangular frame, two groups of parameters are defined: the real frame of category $u$, $v = (v_x, v_y, v_w, v_h)$, and the predicted frame of category $U$, $t^u = (t_x, t_y, t_w, t_h)$. The detailed process is as following.

$$t_x = \frac{x - x_a}{w_a}, t_y = (y - y_a), t_\omega = \log\frac{w}{w_a}, t_h = \log\frac{h}{h_a} \quad (16)$$

where $(x, y, w, h)$ is the center coordinate and frame width and height of the real target traffic sign, and $(x_a, y_a, w_a, h_a)$ is the center coordinate of the candidate area and the width and height of the area. The loss of border regression layer is

$$L_{\mathrm{reg}}\left(t^u, v\right) = \sum \mathrm{Smoth}_{L_i}\left(t_i^v - v_i\right) \quad (17)$$

$$\mathrm{Smoth}_{L_i}(x) = \begin{cases} 0.5\, x^2,\ |x| < 1 \\ |x| - 0.5,\ \text{else} \end{cases} \quad (18)$$

In this paper, a two-stage Faster R-CNN model is used to detect traffic signs after dehazing. First, modify the size of the input image to 1360 × 800, and extract features through the VGG16 network. Then, the feature vectors are introduced into the RPN layer and the ROI Pooling layer for multi-scale prediction. Finally, the fully connected layer and the softmax function are used to classify and output the detection results.

### *C. MODEL OF DRIVING SIGHT DISTANCE IN HAZE ENVIRONMENT*

Driving sight distance refers to the longest distance that a driver can continuously see obstacles at a certain height in the lane in front of the road. Or see the traffic facilities and road markings in front of the road from the normal driving position [36]. Safe driving sight distance refers to the minimum distance to take timely measures to prevent traffic accidents,

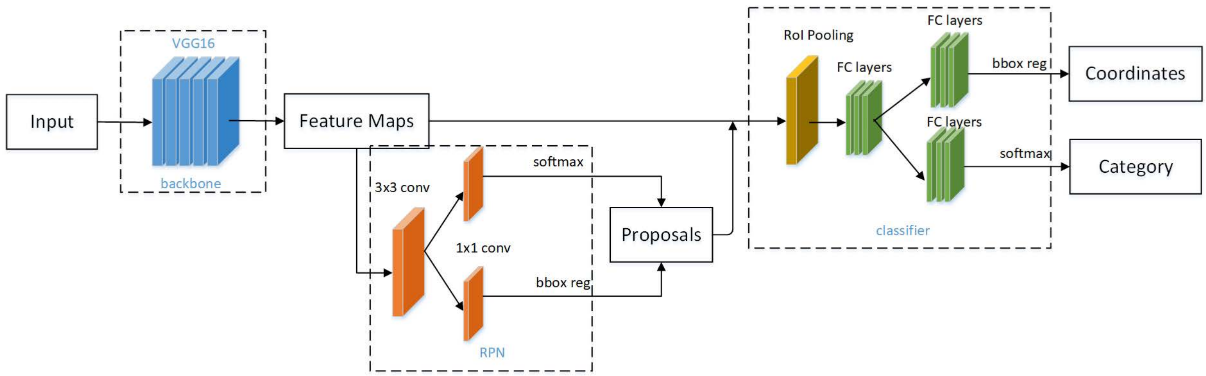


**FIGURE 3.** Faster R-CNN algorithm detection flow chart.

including reaction distance, braking distance and safe parking distance [37]. The process of visual recognition of traffic signs by vehicles is presented in the following Figure 4.

In the figure, $L1$, $L2$, $L3$, $L4$, $L5$ are the identification distance, reading distance, decision-making distance, adjustment distance and safety distance, respectively. The sight distance involved in this article refers to the distance range from the visual recognition point to the point where the traffic sign is located.

In the haze environment, the visibility is reduced, the line of sight is blocked, and the visible distance is shortened. At the same time, due to the scattering and absorption of light, the brightness of objects is decreased, making it difficult to detect and identify traffic signs, which bring security risks. Consult data [38] to get the relationship between road haze and sight distance.As shown in Table 2.

**TABLE 2.** Relationship between visibility, haze level and sight distance.

| type | Visibility (m) | sight distance (m) |
|---|---|---|
| light haze | <1000 | 300∼500 |
| haze | 200∼500 | 50∼150 |
| dense haze | 50∼200 | <50 |

It can be seen from Table 2 that there is a correlation between the driving sight distance and the haze level in haze environment. They affect the detection performance of traffic signs. Therefore, a UV correlation model between the sight distance, haze and traffic sign detection performances is established. As showing in Figure 5.

As showed in Figure 5, in the established correlation model, the U layer is the sight distance layer. $L$, $M$, and $S$ represents long, medium, and short sight distance, respectively. The V layer is the traffic sign detection accuracy, and its value is divided into three grades $A$, $B$, and $C$ according to the experimental results. $W$ is the weight, and its value depends on the haze. The relationship matrix of this model is given in Table 3.

**TABLE 3.** Relationship matrix of related models.

| | A | B | C |
|---|---|---|---|
| L | W11 | W12 | W13 |
| M | W21 | W22 | W23 |
| S | W31 | W32 | W33 |

## III. EXPERIMENT AND ANALYSIS

This article relies on the implementation of python and deep learning theory Tensorflow framework. The hardware configuration is: 12th Gen Intel(R) Core(TM) i5-12400F 2.5 GHZ, CPU memory is 32GB,GPU is NVIDIA GeForce RTX 3060. The operating system is win10, and the development platform is Visual Studio 2017.

### A. DATA PREPROCESSING

The paper uses the German Traffic Signs Dataset (GTSDB)(URL:http://benchmark.ini.rub.de/?section = gtsdb &subsection=dataset) for performance training and testing, which include 600 training images and 300 testing images. In the experiments, two objects, cars and traffic signs, were marked. Most of the images were taken in good lighting and no haze. To obtain images in haze environments, image haze synthesis processing is performed on the dataset. Three different levels of haze images (light haze, haze, and dense haze) are synthesized in the experiments. It simulates the image of the road environment visually received by an autonomous vehicles in a hazy environment. Affected by haze, the clarity of traffic signs observed at different sight distances is different. Referring to Section II.C above, setting the sight distance thresholds of light haze, haze and dense haze to 300, 100 and 50 meters, corresponds to long, medium and short sight distances.

Clarity of traffic signs varies greatly due to different haze levels. When the distance between the image capture point and the traffic sign is constant, the observed sharpness of the traffic sign in light haze conditions is higher than that in haze and dense haze conditions. However, due to the different degree of interference of haze on the sight distance, visual distance and the detection performance of traffic signs

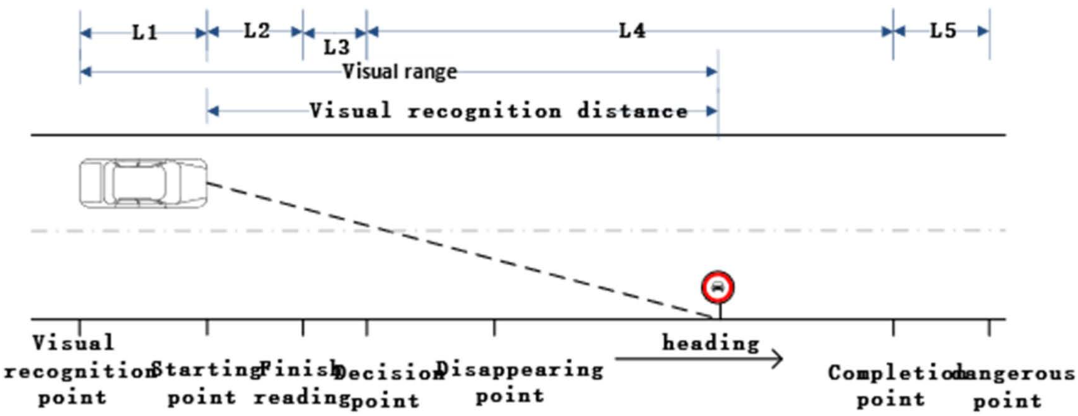


**FIGURE 4.** The process of vehicle recognition of traffic signs.

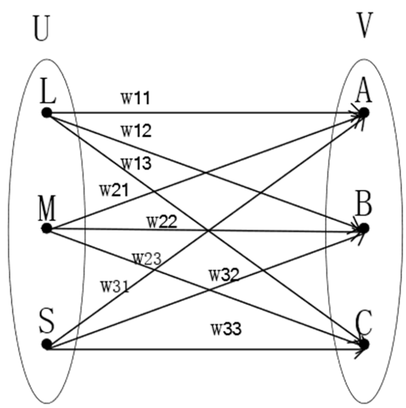


**FIGURE 5.** Correlation model of sight distance, haze and traffic sign detection performance.

under different levels of haze are also different. As showed in Figure 6, when the distance between the autonomous vehicles and the traffic sign is 50 meters, the traffic sign can be observed in all three types of haze. When the distance between the vehicle and the traffic sign is about 100 meters, the visual distance in the dense haze environment is limited, and no traffic signs 50 meters away can be observed. Therefore, it cannot be detected. When the distance between the shooting point and the traffic sign exceeds the visible distance threshold, the traffic sign cannot be detected and recognized.

In this paper, guided filtering dehazing and Faster R-CNN model are used for research. The purpose is to explore the change rule of traffic sign detection performance in different haze environments, so as to ensure the safety of autonomous vehicles in haze environments. In this experiment, guided filtering dehazing algorithm is used to dehaze datasets with different haze. Then, based on different sight distances, the traffic sign data set is trained. In this model, VGG-16 is used as a shared convolutional neural network, and features are transferred to RPN network for secondary classification. At the same time, they are aggregated to produce the feature map of the candidate region. Finally, classification and regression are carried out to detect the category and location of the object. During the experiment, we set the parameters as follows: the weight attenuation is 0.0005, the initial learning rate is 0.001, and it is 1/10 of the initial value after 5000 iterations, totally 10000 iterations. The momentum coefficient in random descent is 0.9.

### B. EXPERIMENTAL RESULTS AND ANALYSIS

#### 1) EVALUATION INDEX

Average precision AP (Average Precision) and mAP (meanAP) are used as training evaluation metrics. AP is the average of the precision values at different recall rates. It reflects the learning performance of the model in different categories.Its calculation formula is as follows.

$$AP = \frac{1}{\mathrm{N}} \sum_{1}^{\mathrm{N}} \mathrm{P} \tag{19}$$

where N represents the total number of input pictures. P indicates the classifier's ability to distinguish between positive and negative samples, that is, precision.

MAP is the average value of AP, and the performance of the model is further measured on the premise of AP. Its calculation formula is as follows.

$$\mathrm{mAP} = \frac{\sum_{1}^{\mathrm{N}} \mathrm{AP}}{\mathrm{N(\ classes\ )}} \mathrm{P} \tag{20}$$

where N(classes) represents the total number of classes.

#### 2) PERFORMANCE OF GTSDB IN HAZE

Object detection algorithm mainly include one-stage and two-stage algorithms. Among them, SSD, YOLO and Retinanet are typical in one-stage object detection. Typical algorithms in two-stages include SPPnet, Faste RCNN and R-FCN. Train these six algorithms on the same data set and system, compare their performance and computational cost. The experimental results are shown in Table 4. The values in the table are the average values of experimental results under light haze, haze and dense haze.

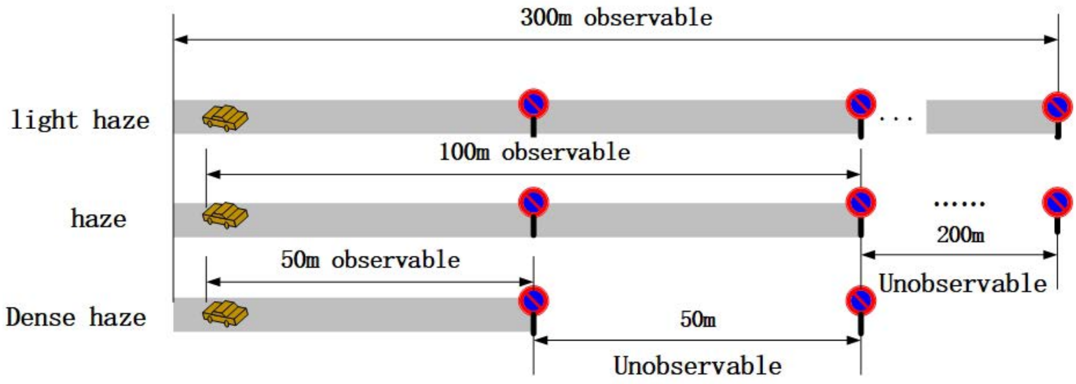


**FIGURE 6.** Comparison of visual distance with different haze.

**TABLE 4.** Algorithm performance comparison.

| | accuracy_haze-free(%) | accuracy_haze(%) | map | test time(s) | train time(s) |
|---|---|---|---|---|---|
| One-stage: | | | | | |
| RetinaNet [39] | 89.76 | 76.49 | 72.88 | 3.95 | 5.68 |
| YOLOX [40] | 92.43 | 79.85 | 78.22 | 6.94 | 9.01 |
| SSD [41] | 93.23 | 83.50 | 74.99 | 2.51 | 3.97 |
| Two-stage: | | | | | |
| R-FCN [42] | 90.77 | 82.69 | 75.58 | 3.4 | 7.34 |
| SPPnet [43] | 89.96 | 80.58 | 74.32 | 9.14 | 12.93 |
| Fater RCNN [44] | 94.18 | 83.87 | 78.36 | 4.53 | 9.04 |

According to the data in the table, on the same hardware and software platform, the Fater RCNN model shows excellent performance in terms of accuracy, calculation time cost and mAP.

The Fater RCNN model is used to train traffic signs with three different haze levels, and the specific experimental results are shown in Table 5.

**TABLE 5.** Training results different grade.

| visibility range | Long sight distance | Medium sight distance | Short sight distance |
|---|---|---|---|
| sight distance (meters) | 300 | 100 | 50 |
| AP of Car (%) | 78.81 | 80.34 | 84.89 |
| AP of Traffic sign ( %) | 78.20 | 77.19 | 70.20 |
| MAP (%) | 78.51 | 78.76 | 77.55 |

Under the three haze conditions, the PR curves trained by the Faster R-CNN model are shown in the following Figure 7.

Combining the above chart and comparing the experimental data of model training, it can be seen that in the haze environment, the AP value of traffic sign detection of different sight distances is above 77%, and the average mAP value is above 78%. The three models achieved high accuracy on AP and mAP, indicating that the model has good training effect and learning performance under three sight distances. In addition, to verify the recognition effect and performance of the trained model on traffic sign images with different sight distances, the images in the test set are tested.It can be observed in the test result graph that when the haze level increases, the visual distance of the autonomous vehicles becomes shorter due to the increase of line-of-sight interference. At the same time, the detection performance of the model on traffic sign images decreases. When the haze increases and the traffic sign image observation distance is long, false detection and missed detection may occur. Part of missed detection and false detection results are shown in Figure 8.

Haze and dehazed datasets are tested at three different sight distances: long, medium and short. The test results for the test set are sorted out, as showed in Table 6.

**TABLE 6.** Test dataset results.

| Visibility range | 300 m (Light haze) | | 100 m (Haze) | | 50 m (Dense haze) | |
|---|---|---|---|---|---|---|
| | Haze image | After dehaze | Haze image | After dehaze | Haze image | After dehaze |
| Accuracy (%) | 85.11 | 95.75 | 84.75 | 93.99 | 81.76 | 92.81 |
| Loss(%) | 2.03 | 0.45 | 3.04 | 0.45 | 6.52 | 0.48 |
| False detection rate (%) | 19.19 | 1.35 | 25.57 | 1.58 | 40.48 | 1.90 |

The Figure 9 shows the distribution of model test accuracy under three haze conditions.

It can be observed in the normal probability diagram that detection accuracy under the three haze environments is concentrated between 0.9 and 1, indicating that the detection performance of this experiment is excellent. Experimental results of comparison of dehazing performance. Under the condition of light haze, the threshold of sight distance is 300 meters, and the recognition rate of hazy images is 85.11%. The image recognition rate after filtering and dehazing algorithm is 95.75%. After dehazing, the recognition

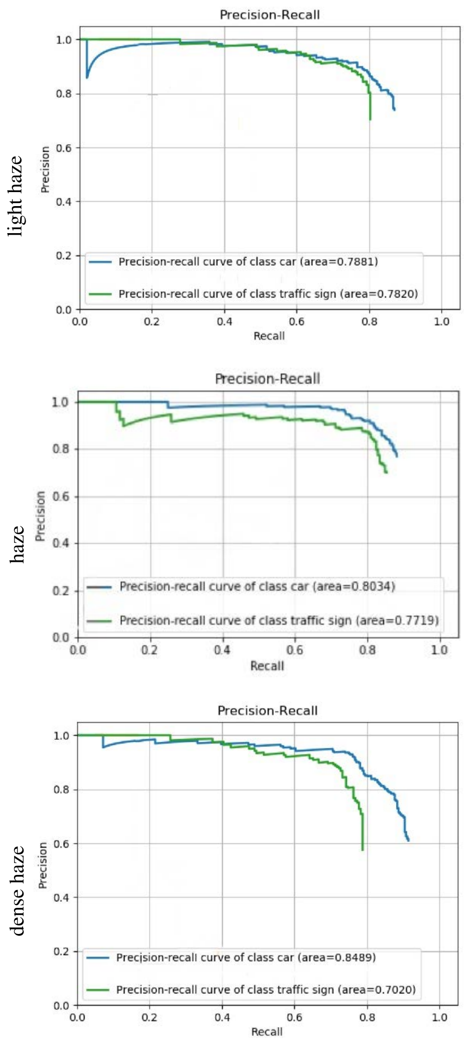


**FIGURE 7.** **The PR curves trained by the faster R-CNN.**

efficiency is improved by 10.64%. The missed detection rate and false detection rate of hazy images are higher than those of traffic sign images after dehazing. The false detection rate of the hazed image is 14 times that of the dehazed image. Under the condition of haze, the threshold of sight distance is 100 meters, and the traffic sign recognition detection rate of dehazed images is as high as 93.99%. Under the same conditions, the detection rate of hazy image is only 84.75%, which is lower than 9.24% of haze-free image. The missed detection rate and false detection rate of haze images are 6.75 times and 16 times that of dehazed images, respectively. Under the condition of dense haze, the shortest threshold of sight distance is 50 meters. After dehazing, the detection and recognition rate is 92.81%, while the hazy image is 81.76%. The missed detection rate and false detection rate of haze images are 13.58 times and 21.31 times that of dehazed images respectively.To sum up, the experiment shows that the detection results of traffic signs are greatly affected by haze. The tilt angle, shooting distance and height of the image have no obvious influence on the experimental results.

According to the experimental results of Faster R-CNN model, three training models with different sight distance thresholds are obtained. Under different models, three kinds of environmental traffic sign images are detected: light haze, haze and dense haze. The variation trend of the accuracy, missed detection rate and false detection rate of this experiment is shown in Figure 10.

Comparing the three index values before and after dehazing in Figure 10, it can be seen that the traffic sign detection experiment after dehazing is obviously better than that before dehazing, which verifies the effectiveness of this image haze removal experiment from the side. Comparing the visual results of long, medium and short horizontal sight distances, it shows that the missed detection rate and false detection rate are obviously the lowest and the detection accuracy rate is the highest when the sight distance is far away. In the case of short sight distance, the evaluation value of each index is the worst. Figure 10 shows the horizontal and vertical comprehensive evaluation, it can be seen that in the detection performance of traffic sign images with different sight distances, the haze-containing image and the image after dehazing have similar laws. The detection accuracy decreases with the shortening of the sight distance, while the false detection rate and the missed detection rate increase with the shortening of the sight distance. The detection accuracy of dense haze images is abnormal. The reason is that when the haze is too heavy, the line-of-sight interference will be strengthened, and the missed detection rate and false detection rate of traffic signs will increase. Only traffic signs within the visible range can be detected, and the detection accuracy is correspondingly improved.

### 3) SOLVING AND ANALYSIS OF CORRELATION MODEL BASED ON KM ALGORITHM

Different haze environments have distinct effects on the driving sight distance. Therefore, w values were determined to be 3, 2 and 1 under light haze, haze and dense haze conditions, respectively. According to the experimental results of traffic sign detection in haze environment, the accuracy rate of more than 93% is grade A, and the value ranges of grade B and grade C are 88%-93% and 85%-88%, respectively. When there is a conflict between weighted paths, the path with the larger weight is expected to be adopted. Then the relational matrix of the relational model is shown in Table 7.

**TABLE 7.** **The relationship matrix is obtained through experiments.**

| | A | B | C |
|---|---|---|---|
| L | 3 | 2 | 0 |
| M | 0 | 3 | 2 |
| S | 0 | 3 | 1 |

Given the UV correlation model in the sorted state, it is abstracted into two point sets U and V. The points $U_i$ and $V_j$ in U and V represent the i-th row and j-th column in Table 2, respectively. $l(i, j)$ represents the edge connecting $U_i$ and $V_j$. The weight $\omega(i, j)$ here is the number of incompatible

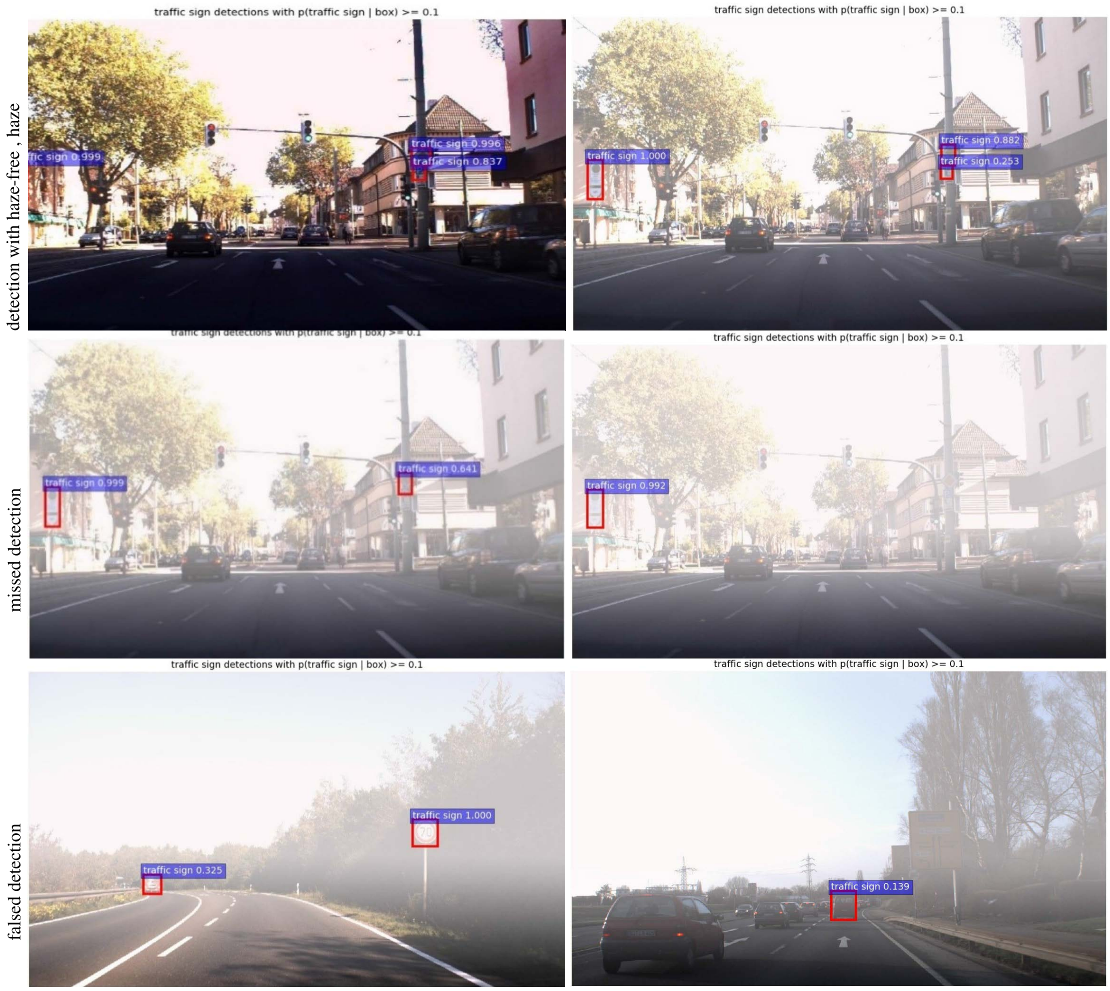


**FIGURE 8.** Schematic diagram of part of the test results.

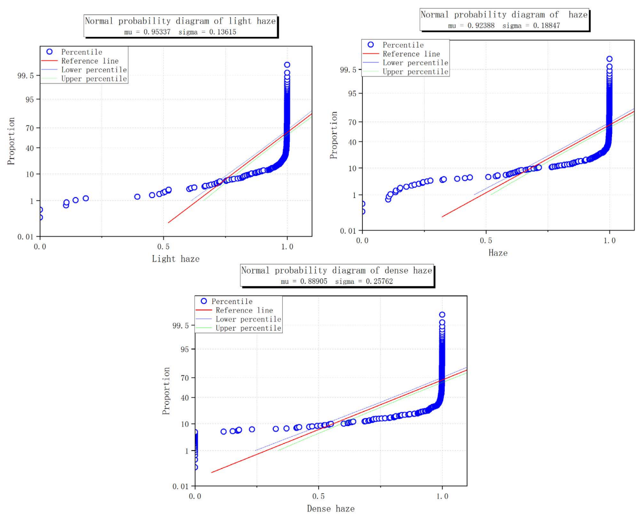


**FIGURE 9.** Test set statistics under different haze.

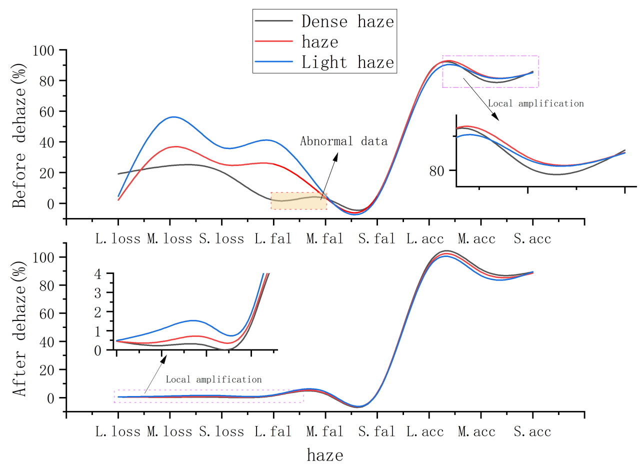


**FIGURE 10.** Test accuracy results under different sight distance conditions.

digits between $U_i$ and $V_j$, indicating the "detection accuracy" required to put the vector in the i-th row in the UV model into the j-th row. The problem of increasing the correlation between the test set and the principal component matrix is transformed into the complete matching problem of bipartite

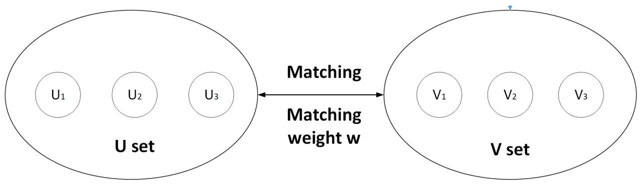


**FIGURE 11.** Bipartite graph matching model.

graph [45], which requires the highest matching "detection accuracy". KM (Kuhn-Munkras) algorithm [46] is used to find an exact match and adjust the order of test sets according to the information contained in the match. KM algorithm, as an algorithm for solving bipartite matching, introduces the concepts of feasible vertex and equal subgraph compared with Hungarian algorithm [47], thus completing greedy expansion of Hungarian algorithm [48] and obtaining the best complete matching. The whole process of the algorithm is as follows.

*Step1:* initializing the value of the feasible bid; It is stipulated that $l_u(u)$ and $l_v(v)$ respectively record the top label values of nodes in sets u and v. Initially, the value of $l_u(u_i)$ is set as the maximum weight $\omega(u_i, v_i)$ of the edge $e(u_i, v_i)$ associated with $u_i$, so that $l_v(v_i) = 0$ and $l_u(u_i) + l_v(v_i) \leq \omega(u_i, v_i)$.

*Step 2:* Find the complete matching of equal subgraphs by Hungary algorithm; Hungary uses the augmented path to find the maximum match, and by finding an augmented path $p$, a larger match is obtained in the inversion operation to replace the initial match until the augmented path cannot be found.

*Step 3:* Modify the value of the feasible bid; For the visited vertex $u$, subtract $d$ from its feasible vertex.

$$d = \min_{U \in S, V \in B} \{l(u) + l(v) - \omega(u, v)\} \tag{21}$$

While the feasible top marks of all visited vertices v are increased by d, where S $\subseteq$ U,B $\subseteq$ V

*Step 4:* Repeat Step 2 and Step 3 until you find an equal subgraph that matches perfectly.

The KM algorithm is used to solve the optimal matching of the Correlation models, and the results are shown in Figure 12.

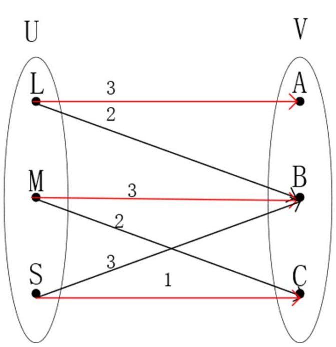


**FIGURE 12.** Best matching results for correlation model.

The red arrow in the figure is the matching result of the KM algorithm. According to the results of the KM algorithm, when the sight distance is long, medium, and short, the accuracy levels of traffic sign detection are A, B, and C, respectively.

Comprehensive analysis shows that in the dense haze environment, when the sight distance is less than 50 meters, the situation around the road is difficult to distinguish due to the serious interference of the sight line, and it is easy to miss the road traffic signs. In addition to the high false detection rate and missed detection rate, the detection accuracy rate of traffic signs is also very low, only Class C, which is likely to bring serious security risks to themselves and other traffic participants. In the haze environment, there will be missed detection and false detection, but the average detection accuracy of traffic signs is higher than that in the fog environment. In the light haze environment, when the sight distance threshold is 300 meters, the missed detection rate and false detection rate are low, and the traffic sign detection effect level reaches Grade A. Under the condition of A, the autonomous vehicles has the best effect on traffic sign recognition, and its safety is higher than that of B and C.

## IV. CONCLUSION AND PROSPECTS

The research focus of this paper is to explore the influence of different driving sight distance on traffic sign detection in haze environment. The difficulty lies in how to train and test the traffic sign data set containing haze accurately, and classify it according to the experimental results to build a UV correlation model. The difficulty of this experiment also lies in how to train and test the traffic sign data set containing haze accurately, and classify the experimental results. In this paper, a model of haze removal by combining dark channel prior with guided filtering is adopted. The model greatly enhances the image quality, while avoiding the white edge, halo effect and other undesirable phenomena. The traffic sign detection based on Faster RCNN has achieved good experimental results. Detect traffic signs under different haze levels and sight distances. The results show that with the increase of haze and the shortening of sight distance, the accuracy of traffic signs is lower, and the false detection rate and missed detection rate are higher, which reduces the travel safety in the haze environment. The established UV correlation model can well explore the relationship among haze, traffic signs and sight distance threshold. KM algorithm is used to solve the UV correlation model, and it is concluded that under the conditions of light haze, haze and dense haze, the detection effects of traffic signs are Grade A, B and C respectively. It shows that with the increase of haze, the safety of self-driving vehicles decreases. In this paper, experiments are carried out on the data set of traffic signs with and haze-free, and two conclusions are verified: the detection effect of traffic signs after haze removal is better than that of images with haze, and haze and sight distance have significant influence on traffic sign detection. This paper mainly considers the influence of haze level and sight distance on the detection effect of traffic signs. Follow-up research can start with the relationship between vehicle speed and sight distance in haze environment, and build the recognition and detection effect of traffic signs under the comprehensive relationship model of different haze levels, driving speed and sight distance threshold.The validity and feasibility of the model in the real-time scene in the field of transportation has great research value and practical significance, and this part of the content can be discussed as the focus in the follow-up research.

## REFERENCES


[1] *Road Traffic Signs and Markings Part I: General Principles, GB5768.1-2009*, State Bureau of Quality and Technical Supervision, Beijing, China, 2009.

[2] D. Tabernik and D. Skocaj, "Deep learning for large-scale traffic-sign detection and recognition," *IEEE Trans. Intell. Transp. Syst.*, vol. 21, no. 4, pp. 1427–1440, Apr. 2020.

[3] C. Wang, "Research and application of traffic sign detection and recognition based on deep learning," in *Proc. Int. Conf. Robots Intell. Syst. (ICRIS)*, May 2018, pp. 150–152.

[4] G. Yuanyuan, "Small and dense traffic sign detection in autonomous driving environment," *J. Intell. Syst.*, vol. 13, no. 3, pp. 366–372,2018.

[5] Q. Xiao and W. Yu, "Traffic sign detection in complex environment based on improved YOLOv3," *Int. Core J. Eng.*, vol. 7, no. 3, pp. 102–108, 2021.

[6] H. W. Arman, A. Samin, and H. M. Abul, "DeepThin: A novel lightweight CNN architecture for traffic sign recognition without GPU requirements," *Expert Syst. Appl.*, vol. 168, Apr. 2021, Art. no. 114481.

[7] A. Hechri and A. Mtibaa, "Two-stage traffic sign detection and recognition based on SVM and convolutional neural networks," *IET Image Process.*, vol. 14, no. 5, pp. 939–946,2020.

[8] H. Wang, R. Yuan, H. Pan, W. Liu, Z. Xing, and J. Huang, "Speed sign recognition in complex scenarios based on deep cascade networks," *IET Intell. Transp. Syst.*, vol. 14, no. 6, pp. 628–636, Jun. 2020.

[9] J. Zhang, Z. Xie, J. Sun, X. Zou, and J. Wang, "A cascaded R-CNN with multiscale attention and imbalanced samples for traffic sign detection," *IEEE Access*, vol. 8, pp. 29742–29754, 2020.

[10] J. Li and Z. Wang, "Real-time traffic sign recognition based on efficient CNNs in the wild," *IEEE Trans. Intell. Transp. Syst.*, vol. 20, no. 3, pp. 975–984, Mar. 2019.

[11] Á. Arcos-García, J. A. Álvarez-García, and L. M. Soria-Morillo, "Deep neural network for traffic sign recognition systems: An analysis of spatial transformers and stochastic optimisation methods," *Neural Netw.*, vol. 99, pp. 158–165, Mar. 2018.

[12] D. Li, D. Zhao, Y. Chen, and Q. Zhang, "DeepSign: Deep learning based traffic sign recognition," in *Proc. Int. Joint Conf. Neural Netw. (IJCNN)*, Jul. 2018, pp. 1–6.

[13] C. Lin, L. Li, W. Luo, K. C. P. Wang, and J. Guo, "Transfer learning based traffic sign recognition using inception-v3 model," *Periodica Polytechnica Transp. Eng.*, vol. 47, no. 3, pp. 242–250, Aug. 2018.

[14] C. Zhang, X. Yue, R. Wang, N. Li, and Y. Ding, "Study on traffic sign recognition by optimized Lenet-5 algorithm," *Int. J. Pattern Recognit. Artif. Intell.*, vol. 34, no. 1, Jan. 2020, Art. no. 2055003.

[15] S.-K. Tai, C. Dewi, R.-C. Chen, Y.-T. Liu, X. Jiang, and H. Yu, "Deep learning for traffic sign recognition based on spatial pyramid pooling with scale analysis," *Appl. Sci.*, vol. 10, no. 19, p. 6997, Oct. 2020.

[16] Z. Liu, J. Du, F. Tian, and J. Wen, "MR-CNN: A multi-scale region-based convolutional neural network for small traffic sign recognition," *IEEE Access*, vol. 7, pp. 57120–57128, 2019.

[17] S. Aziz, E. A. Mohamed, and F. Youssef, "Traffic sign recognition based on multi-feature fusion and ELM classifier," *Proc. Comput. Sci.*, vol. 127, pp. 146–153, Jan. 2018.

[18] Z. Nadeem, Z. Khan, U. Mir, U. I. Mir, S. Khan, H. Nadeem, and J. Sultan, "Pakistani traffic-sign recognition using transfer learning," *Multimedia Tools Appl.*, vol. 81, no. 6, pp. 8429–8449, Mar. 2022.

[19] J. Cao, J. Zhang, and X. Jin, "A traffic-sign detection algorithm based on improved sparse R-CNN," *IEEE Access*, vol. 9, pp. 122774–122788, 2021.

[20] K. Ren, L. Huang, C. Fan, H. Han, and H. Deng, "Real-time traffic sign detection network using DS-DetNet and lite fusion FPN," *J. Real-Time Image Process.*, vol. 18, no. 6, pp. 2181–2191, Dec. 2021.

[21] C. Hodges, "Deep learning based vision for driverless vehicles in hazy environmental conditions," Univ. Western Australia, Perth, WA, Australia, 2021.

[22] G. Yan, M. Yu, S. Shi, and C. Feng, "The recognition of traffic speed limit sign in hazy weather," *J. Intell. Fuzzy Syst.*, vol. 33, no. 2, pp. 873–883, Jul. 2017.

[23] C. Xiuxin, Y. Yang, and Y. Zhong, "Traffic sign recognition in hazegy weather based on deep learning," *J. Chongqing Jiaotong Univ. (Natural Sci. Ed.)*, vol. 39, no. 12, 2020.

[24] T. Wiesemann and X. Jiang, "Fog augmentation of road images for performance analysis of traffic sign detection algorithms," in *Proc. Int. Conf. Adv. Concepts Intell. Vis. Syst.* Cham, Switzerland: Springer, 2016, pp. 685–697.

[25] R. Belaroussi and D. Gruyer, "Impact of reduced visibility from fog on traffic sign detection," in *Proc. IEEE Intell. Vehicles Symp.*, Jun. 2014, pp. 1302–1306.

[26] L. Ma, Q. Wu, Y. Zhan, B. Liu, and X. Wang, "Traffic sign detection based on improved YOLOv3 in foggy environment," in *Proc. Int. Conf. Wireless Commun., Netw. Appl.*, 2022, pp. 685–695.

[27] R. Anthony and J. Biswas, "Real-time traffic sign detection under foggy condition," in *Sustainable Advanced Computing*. Singapore: Springer, 2022, pp. 137–144.

[28] J. Xing and W. Q. Yan, "Traffic sign recognition using guided image filtering," in *Proc. Int. Symp. Geometry Vis.*, 2021, pp. 85–99.

[29] R. Belaroussi and D. Gruyer, "Convergence of a traffic signs-based fog density model," in *Proc. IEEE 18th Int. Conf. Intell. Transp. Syst.*, 2015.

[30] Z. Xu and M. Chen, "Modified image dehazing algorithm of traffic sign image in fog and haze weather," *J. Comput. Appl.*, vol. 37, no. 8, p. 2329, 2017.

[31] C. Deng, "Using the QN-ACTR cognitive architecture to simulate the effect of limited line-of-sight on car-following performance in fog," *Traffic Res. F: Traffic Psychol. Behav.*, vol. 65, pp. 643–654, Jan. 2019.

[32] P. Discetti and R. Lamberti, "Traffic sign sight distance for low-volume roads," *Transp. Res. Rec., J. Transp. Res. Board*, vol. 2203, no. 1, pp. 64–70, Jan. 2011.

[33] K. He, J. Sun, and X. Tang, "Single image haze removal using dark channel prior," *IEEE Trans. Pattern Anal. Mach. Intell.*, vol. 33, no. 12, pp. 2341–2353, Dec. 2011.

[34] K. He, J. Sun, and X. Tang, "Guided image filtering," in *Proc. Eur. Conf. Comput. Vis.* Berlin, Germany: Springer, 2010, pp. 1–14.

[35] C. Ying, M. Qi-Guang, L. Jia-Chen, and G. Lin, "Advance and prospects of AdaBoost algorithm," *Acta Automatica Sinica*, vol. 39, no. 6, pp. 745–758, 2013.

[36] Z. Lixia and Y. J. Shun, *Traffic Safety Engineering*. China: Machinery Industry Press, 2018, p. 14.

[37] Z. Haitai *et al.*, "Research on variable speed limit control strategy for short-circuit sections in bridge and tunnel group areas based on safe driving sight distance," *Highway Traffic Technol., Appl. Technol. Ed.*, vol. 4, no. 8, pp. 260–263, 2019.

[38] *Specification for Design of Highway LinesJtd 2004–2017*, Ministry of Transport, Beijing, China, 2017.

[39] T.-Y. Lin, P. Goyal, R. Girshick, K. He, and P. Dollar, "Focal loss for dense object detection," *IEEE Trans. Pattern Anal. Mach. Intell.*, vol. 42, no. 2, pp. 318–327, Feb. 2020.

[40] Z. Ge *et al.*, "YOLOX: Exceeding YOLO series in 2021," 2021, *arXiv:2107.08430*.

[41] W. Liu, D. Anguelov, and D. Erhan, "SSD: Single shot multibox detector," in *Proc. Eur. Conf. Comput. Vis.*, 2015, pp. 21–37.

[42] J. Dai, Y. Li, K. He, and J. Sun, "R-FCN: Object detection via region-based fully convolutional networks," in *Proc. Adv. Neural Inf. Process. Syst.* Red Hook, NY, USA: Curran Associates, 2016, pp. 1–9.

[43] K. He, X. Zhang, S. Ren, and J. Sun, "Spatial pyramid pooling in deep convolutional networks for visual recognition," *IEEE Trans. Pattern Anal. Mach. Intell.*, vol. 37, no. 9, pp. 1904–1916, Sep. 2015.

[44] S. Ren, K. He, R. Girshick, and J. Sun, "Faster R-CNN: Towards real-time object detection with region proposal networks," *IEEE Trans. Pattern Anal. Mach. Intell.*, vol. 39, no. 6, pp. 1137–1149, Jun. 2017.

[45] D. B. H. Tay and J. Zhang, "Techniques for constructing biorthogonal bipartite graph filter banks," *IEEE Trans. Signal Process.*, vol. 63, no. 21, pp. 5772–5783, Nov. 2015.

[46] H. Liangliang, "A nonintrusive recognition method of household load behavior based on DTW algorithm," *Electr. Meas. Instrum.*, vol. 56, no. 14, pp. 17–22, 2019.

[47] X. M. Zhao, D. Fang, and K. J. Mao, "An optimization method for WSN barrier gap repair," *Chin. J. Sens. Actuators*, vol. 31, no. 10, pp. 1566–1572, 2018.
[48] E. W. Wei, W. H. Li, Z. H. Zhang, and J. Zheng, "A non-intrusive load matching method based on improved Hungarian algorithm," *Electr. Meas. Instrum.*, vol. 56, no. 22, pp. 58–64, 2019.

**RONG HU** was born in Sichuan, China, in June 1998. She received the bachelor's degree in transportation from Xihua University, in 2020, where she is currently pursuing the graduate degree. Her research interest includes traffic safety engineering, including self-driving vehicles and image recognition and detection.

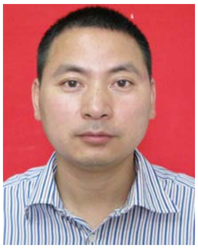

**HUI LI** received the bachelor's degree in surveying and mapping engineering (photogrammetry and remote sensing) and the master's degree in transportation planning and management from Southwest Jiaotong University, in 2000 and 2005, respectively. He is an Associate Professor. He presided over more than 20 traffic planning projects, such as "the belt and road initiative" and six traffic safety projects, and was responsible for the long-term judicial appraisal of major road traffic accident cases. His research interests include road traffic planning, traffic big data, intelligent network traffic signs, and the impact of road traffic operation. He is a member of the Expert Group of Sichuan Road Traffic Safety Association and a Traffic Safety Expert of the Sichuan Emergency Management Department.

**DAN HUANG** was born in Sichuan, China, in October 1998. She received the bachelor's degree in transportation from Xihua University, in 2020, where she is currently pursuing the postgraduate degree. Her research interest includes traffic planning. She won the First Prize and the Second Prize of the Postgraduate Scholarship.

**XIAOJIN XU** born in 1998. She received the bachelor's degree in traffic engineering from Xihua University, in 2020, where she is currently pursuing the postgraduate degree. Her research interest includes traffic information engineering and control.

**KUANGYUAN HE** was born in 1998. He received the bachelor's degree in traffic engineering from Xihua University, in 2020, where he is currently pursuing the postgraduate degree. His research interest includes traffic safety engineering.